Dalton Transactions

COMMUNICATION

View Article Online
View Journal | View Issue

Cite this: *Dalton Trans.*, 2015, **44**, 2052

Received 15th August 2014,
Accepted 5th December 2014

DOI: 10.1039/c4dt02491e

www.rsc.org/dalton

Synthesis and characterization of bimetallic metal–organic framework Cu–Ru-BTC with HKUST-1 structure†

Meike A. Gotthardt,[a] Roland Schoch,[b] Silke Wolf,[c] Matthias Bauer*[b] and Wolfgang Kleist*[a,d]

The bimetallic metal–organic framework Cu–Ru-BTC with the stoichiometric formula $Cu_{2.75}Ru_{0.25}(BTC)_2{\cdot}xH_2O$, which is isoreticular to HKUST-1, was successfully prepared in a direct synthesis using mild reaction conditions. The partial substitution of Cu^{2+} by Ru^{3+} centers in the paddlewheel structure and the absence of other Ru-containing phases was proven using X-ray absorption spectroscopy.

In recent years, metal–organic frameworks (MOFs) have attracted increasing interest for various applications due to their unique properties.[1,2] The copper-based framework HKUST-1[3], also known as MOF-199[4] or Cu-BTC, in which dimeric Cu^{2+} units are bridged by benzene-1,3,5-tricarboxylate (BTC) linkers, represents one of the most prominent and best-studied examples of this class of materials. Both copper centers in the resulting paddlewheel structure feature a coordinated water molecule in axial position, which can either be replaced by substrate molecules or be removed by thermal treatment therefore generating potential binding sites for small molecules. Consequently, various applications of HKUST-1 in the fields of gas storage[5–7] or catalysis have been reported. For example Cu-BTC exhibited high catalytic activity in Knoevenagel condensation reactions,[8] Friedländer quinoline synthesis[9] as well as in other CC bond-forming reactions.[10]

Although these examples nicely illustrate the potential of Cu-BTC, various efforts have been made to overcome some intrinsic handicaps of the HKUST-1 structure. Mixed-linker Cu-BTC-PyDC materials have been synthesized where the BTC ligands have been partially substituted by pyridine-3,5-dicarboxylates (PyDC).[11] This replacement resulted in defect coordination at some copper centers leading to an increased flexibility of the framework on the one hand side and an altered electronic structure on the other. Both effects might have a positive impact on the dynamic processes occurring during catalytic applications. Moreover, linker molecules with an additional side group were used for the synthesis of amine functionalized Cu-BTC.[12] In addition, several other isoreticular M-BTC materials consisting of Fe, Mo, Cr, Ni, Zn and Ru, respectively, have been reported,[5,6,13,14] which opens up possibilities for further applications involving the special adsorption or redox properties of the corresponding metal ions. Recently, a mixed-metal Cu–Zn-BTC has been reported in which small fractions of Cu were replaced by Zn.[15] The incorporation of zinc centers in this structure was confirmed using NMR and EPR spectroscopic studies and the resulting material has been subject of further theoretic as well as spectroscopic studies.[16,17]

In the present work, we have synthesized a mixed-metal Cu–Ru-BTC material using a direct preparation route at ambient pressure based on a method previously reported for Cu-BTC.[11] For comparison, a pure Cu-BTC sample was synthesized. Although an initial Cu : Ru molar ratio of 4 : 1 was applied during synthesis, ICP-OES analysis of the Cu–Ru-BTC sample revealed that 23 wt% of copper but only 3.2 wt% of ruthenium were present in the material. This metal ratio corresponds to a stoichiometric formula of $Cu_{2.75}Ru_{0.25}(BTC)_2{\cdot}xH_2O$, assuming that exclusively an HKUST-like structure is formed in which approximately 8% of the Cu framework centers have been replaced by Ru (Scheme 1). However, it might also be possible that other ruthenium species, *e.g.* small metallic or oxidic clusters or nanoparticles, have been deposited inside a Cu-BTC framework. The resulting material

[a]*Institute for Chemical Technology and Polymer Chemistry, Karlsruhe Institute of Technology (KIT), Engesserstr. 20, 76131 Karlsruhe, Germany*
[b]*Department Chemie, Fakultät für Naturwissenschaften, Universität Paderborn, Warburgerstr. 100, 33098 Paderborn, Germany. E-mail: matthias.bauer@upb.de; Tel: +49 5251 605614*
[c]*Institute for Inorganic Chemistry, Karlsruhe Institute of Technology (KIT), Engesserstr. 15, 76131 Karlsruhe, Germany*
[d]*Institute of Catalysis Research and Technology, Karlsruhe Institute of Technology (KIT), Hermann-von-Helmholtz-Platz 1, 76344 Eggenstein-Leopoldshafen, Germany. E-mail: wolfgang.kleist@kit.edu; Tel: +49 721 60847989*
†Electronic supplementary information (ESI) available: Experimental details, ATR-IR spectra, N_2 adsorption isotherm, ICP-OES and XAS details. See DOI: 10.1039/c4dt02491e

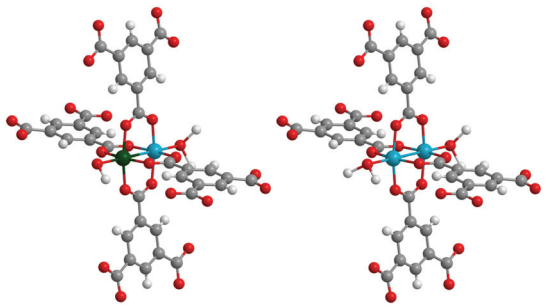

Scheme 1 Structural motifs found in Cu–Ru-BTC; left: Cu–Ru paddlewheel (approx. 16%); right: Cu–Cu paddlewheel (approx. 84%).

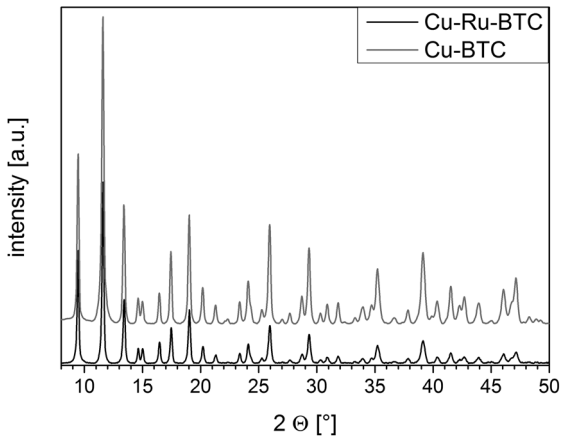

Fig. 1 XRD patterns of Cu–Ru-BTC (black) and Cu-BTC (grey).

was therefore thoroughly characterized to confirm the successful formation of Cu–Ru-BTC *via* incorporation of Ru^{3+} ions in the HKUST-1 framework and the absence of undesired Ru species.

Powder X-ray diffraction measurements of Cu–Ru-BTC (Fig. 1) confirmed that the desired HKUST-1 structure was formed during the synthesis, although the mixed-metal material was less crystalline than the reference Cu-BTC. No contributions of other crystalline phases could be detected in the diffraction pattern, indicating that additional Ru-containing phases were either amorphous, too small to be detected or not present at all.

To exclude the presence of undesired residual precursor species inside the pores, an ATR-IR spectrum of Cu–Ru-BTC was recorded (Fig. S1†). It was identical to the spectrum obtained for Cu-BTC and did not show additional bands from free benzene-1,3,5-tricarboxylic acid molecules indicating that the pores should exclusively contain solvent molecules which can be removed upon thermal activation.

The specific surface area and the accessibility of the pore structure were investigated using nitrogen physisorption measurements (Fig. S2†). While the specific surface area of the Cu-BTC sample (S_{BET}: 1560 m^2 g^{-1}) was similar to values found for HKUST-1 in literature, a significantly lower value of

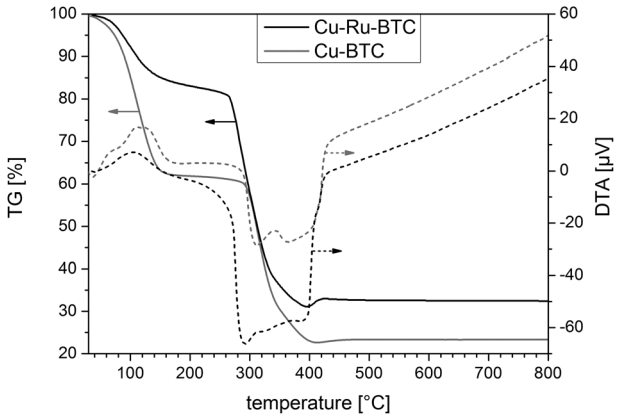

Fig. 2 TG (solid lines) and DTA (dotted lines) curves of Cu–Ru-BTC (black) and Cu-BTC (grey).

570 m^2 g^{-1} was found for Cu–Ru-BTC. Similar observations have been made by Gul-E-Nor *et al.* for mixed-metal Cu–Zn-BTC, where the surface area dropped from more than 1100 m^2 g^{-1} to only 830 m^2 g^{-1} for a sample with a comparatively high Zn content.[15] The authors explained this by possible coordination defects around the zinc centers, which may prevent the full formation of 3D porosity. In addition to this, the larger size difference of Ru^{3+} and Cu^{2+} ions (compared to that of Zn^{2+} and Cu^{2+} ions in Cu–Zn-BTC) might cause an increased disorder of the lattice, which provides a reasonable explanation for the reduced porosity of Cu–Ru-BTC.

Thermogravimetric analysis also supported a reduced porosity of Cu–Ru-BTC (Fig. 2). While a mass loss from water of approx. 35 wt% was observed for pure Cu-BTC in the temperature range <150 °C, only 15 wt% of incorporated water molecules were found in the pores of Cu–Ru-BTC. Furthermore, evaluation of the TG curves of the two materials revealed that the thermal stability of Cu–Ru-BTC was slightly reduced and framework decomposition started earlier (at 265 °C compared to 290 °C for Cu-BTC). This behavior was also confirmed by the shift of the minimum of the DTA curve from 310 °C for Cu-BTC to 290 °C for Cu–Ru-BTC, indicating the maximum rate of thermal decomposition at these temperatures.

Since X-ray absorption spectroscopy (XAS)[18] is a predestinated method for the examination of coordination structures and oxidation states of metal centers in amorphous materials,[19] porous structures[20] and MOFs,[21,22] XAS spectra for the bimetallic Cu–Ru-BTC have been recorded at the K-edges of both Cu and Ru to identify the location and environment of the metal centers in the framework. Information about the oxidation state and the coordination geometry of a metal center can be obtained using XANES (X-ray absorption near edge structure) spectroscopy. For the bimetallic Cu–Ru-BTC spectra of the Cu K-edge (Fig. 3, left, black) and of the Ru K-edge (Fig. 3, right) were recorded. Additionally a spectrum of pure Cu-BTC was recorded at the Cu K-edge (Fig. 3, left, grey) as reference. The Cu K-edge XANES spectra of both samples (Fig. 3, left) do not differ significantly which proves an identical structure at the copper centers for both pure Cu-BTC and

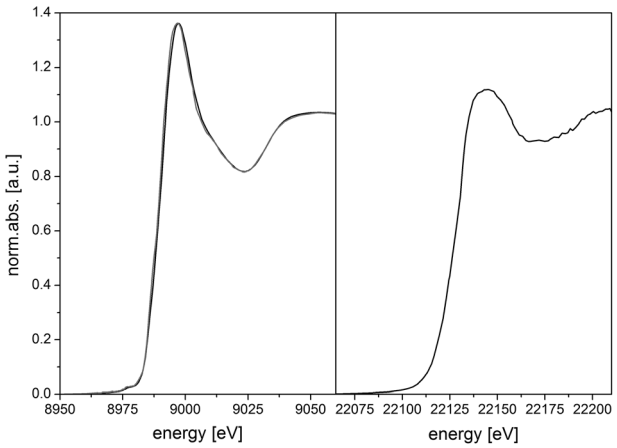

Fig. 3 Normalized X-ray absorption spectra of the copper K-edge (left) of Cu–Ru-BTC (black) and Cu-BTC (grey) and the ruthenium K-edge (right) of Cu–Ru-BTC.

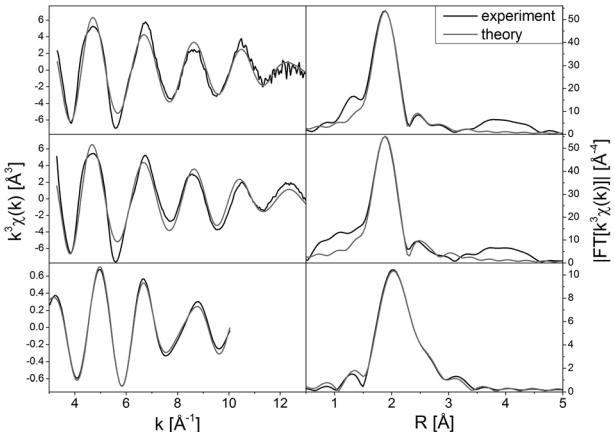

Fig. 4 EXAFS spectra $k^3\chi(k)$ (left) and the corresponding Fourier transformed functions (right) of Cu-BTC (top), Cu–Ru-BTC (Cu K-edge, middle) and Cu–Ru-BTC (Ru K-edge, bottom).

the mixed-metal Cu–Ru-BTC. A prepeak of very low intensity can be found at 8977 eV. Since such small intensities are characteristic of a quadrupole transition, a Cu^{2+} state with d^9 configuration can be concluded.[20,23,24] Moreover the 1s→4p + ligand-to-metal charge transfer shake-down transition, which is visible as a weak shoulder at 8985 eV, supports this interpretation.[25–27]

The resemblance of the modified Cu–Ru-BTC (Fig. 4, middle) and pure Cu-BTC (Fig. 4, top) is also visible in the EXAFS analysis of the Cu K-edge spectra, which offers details about the local structure. The parameters obtained from EXAFS analysis (Table 1) show that in both cases five oxygen atoms are coordinated to the Cu centers at a distance of 1.95 Å. Four of the oxygen atoms can be attributed to the coordinated carboxylate groups of the BTC linker molecules. The fifth oxygen atom originates from a solvent molecule like water, which has a slightly larger distance to the Cu center. However, this second shell could not be resolved. For both samples the second copper atom of the paddlewheel structure is found at a distance of about 2.63 Å, which is in good agreement with crystal structure analysis[3] and data from previous EXAFS analysis[26] for Cu-BTC. In the analysis of Cu–Ru-BTC an additional metal shell at a distance of 2.72 Å could be attributed to a Cu–Ru shell containing 0.1 Ru neighbors. This small value is consistent with the Cu : Ru molar ratio of approximately 11 : 1 found by ICP-OES. It has to be emphasized that this shell is statistically significant, since without the Ru shell the mismatch between experiment and theory (*R*-factor and χ_{red}^2, definition see ESI†) increased. At a larger distance of 2.84 Å four carbon atoms of the carboxylate groups of the linker molecules were detected. The number of carbon backscatterers differed significantly from the expected value. This is due to the higher noise level and the intrinsic backscattering properties of carbon as light backscatterer.

Table 1 EXAFS analysis fitting parameters and results for the spectra of Cu–Ru-BTC and Cu-BTC

Sample	Abs-Bs[a]	*N*(Bs)[b]	*R*(Abs-Bs)[c] [Å]	σ^d [Å]	R^e [%] χ_{red}^{2f} E_f^g [eV] Afac[h]
Cu–Ru-BTC	Ru–O	3.9 ± 0.3	2.071 ± 0.020	0.032 ± 0.003	9.564
Ru-edge	Ru–Cu	1.1 ± 0.1	2.672 ± 0.026	0.089 ± 0.008	1.4013×10^{-6}
	Ru–C	4.1 ± 0.4	2.738 ± 0.027	0.112 ± 0.011	−2.062
					0.4294
Cu–Ru-BTC	Cu–O	4.9 ± 0.2	1.950 ± 0.019	0.077 ± 0.007	31.27
Cu-edge	Cu–Cu	1.3 ± 0.1	2.649 ± 0.026	0.112 ± 0.011	6.0317×10^{-6}
	Cu–Ru	0.1 ± 0.01	2.720 ± 0.027	0.081 ± 0.008	8.350
	Cu–C	5.6 ± 0.5	2.860 ± 0.028	0.112 ± 0.011	0.7878
Cu-BTC	Cu–O	4.7 ± 0.2	1.946 ± 0.019	0.077 ± 0.007	28.48
Cu-edge	Cu–Cu	1.1 ± 0.1	2.624 ± 0.026	0.102 ± 0.010	4.5141×10^{-6}
	Cu–C	3.3 ± 0.3	2.835 ± 0.028	0.074 ± 0.007	7.189
					0.7946

[a] Abs = X-ray absorbing atom, BS = backscattering atom. [b] Number of backscattering atoms. [c] Distance between absorbing and backscattering atom. [d] Debye–Waller-like factor. [e] Fit index. [f] Reduced χ^2 error (considers besides error to experiment the number of independent points and number of varied parameters). [g] Fermi energy, that accounts for the shift between theory and experiment. [h] Amplitude reducing factor.

Due to an edge energy of 22 126 eV and a characteristic whiteline structure the oxidation state of Ru in Cu–Ru-BTC could be determined as Ru^{3+}.[28] In the EXAFS analysis the self-absorption effect is reflected in a comparatively small value of the amplitude reducing factor of 0.4294 (Table 1). Owing to the low Ru concentration EXAFS analysis was only possible to k = 10 $Å^{-1}$ in $\chi(k)$ after Fourier filtering (Fig. 4, bottom). An oxygen shell containing four atoms could be adjusted at a distance of 2.07 Å. This is a slightly longer distance than expected, since the ionic radius of Ru^{3+} is smaller than that of Cu^{2+}. Furthermore, the Ru–Cu distance in the ruthenium K-edge spectrum (2.67 Å) is marginally smaller than in the copper spectrum (2.72 Å). These two effects can be attributed to the low signal to noise level of the ruthenium spectrum. Due to this, a smaller k-range could be used in the fit, causing a loss in resolution. A substitution of the copper by a second ruthenium shell resulted in a strong increase of the error values. Therefore, adjacent Ru sites in the dimers can be excluded, which also means that no other ruthenium containing phases like clusters or nanoparticles could be found within the detection limits of the method. Consequently, the Ru centers have to be incorporated in the lattice structure. The carbon atoms of the linker carboxyl groups are discernible in a distance of 2.73 Å which is also in good agreement with the results at the copper K-edge. In general, the results of the Ru K-edge analysis fit the results of the analysis of the Cu K-edge spectrum very well.

In summary, a new mixed-metal framework Cu–Ru-BTC containing copper as well as ruthenium centers was successfully synthesized at ambient pressure and low reaction temperature (60 °C). X-ray diffractometry and thermogravimetric analysis proved that the new material is isoreticular to the well-known framework HKUST-1 and stable up to 260 °C in air. ICP-OES analysis resulted in a Cu : Ru molar ratio of approximately 11 : 1 in the material corresponding to a stoichiometric formula of $Cu_{2.75}Ru_{0.25}(BTC)_2{\cdot}xH_2O$. X-ray absorption spectroscopy revealed no contributions of other Ru containing phases and confirmed that Ru^{3+} ions were exclusively incorporated into the framework lattice replacing Cu^{2+} in the paddlewheel structure.

The authors thank the synchrotron radiation sources ANKA (Angströmquelle Karlsruhe) in Karlsruhe, Germany, and ESRF (European Synchrotron Radiation Facility) in Grenoble, France, for providing beamtime at the XAS beamline (ANKA) and beamline BM25A (ESRF), respectively. Roland Schoch and Matthias Bauer thank the German ministry for education and research (BMBF) for funding in frame of the project *SusXES* (FKZ05K13UK1).

Notes and references

1 M. Ranocchiari and J. A. van Bokhoven, *Phys. Chem. Chem. Phys.*, 2011, **13**, 6388–6396.
2 A. U. Czaja, N. Trukhan and U. Müller, *Chem. Soc. Rev.*, 2009, **38**, 1284–1293.
3 S. S. Y. Chui, S. M. F. Lo, J. P. H. Charmant, A. G. Orpen and I. D. Williams, *Science*, 1999, **283**, 1148–1150.
4 D. J. Tranchemontagne, J. R. Hunt and O. M. Yaghi, *Tetrahedron*, 2008, **64**, 8553–8557.
5 H. Noei, O. Kozachuk, S. Amirjalayer, S. Bureekaew, M. Kauer, R. Schmid, B. Marler, M. Muhler, R. A. Fischer and Y. Wang, *J. Phys. Chem. C*, 2013, **117**, 5658–5666.
6 C. R. Wade and M. Dinca, *Dalton Trans.*, 2012, **41**, 7931–7938.
7 L. J. Murray, M. Dinca, J. Yano, S. Chavan, S. Bordiga, C. M. Brown and J. R. Long, *J. Am. Chem. Soc.*, 2010, **132**, 7856–7857.
8 M. Opanasenko, A. Dhakshinamoorthy, M. Shamzhy, P. Nachtigall, M. Horacek, H. Garcia and J. Cejka, *Catal. Sci. Technol.*, 2013, **3**, 500–507.
9 E. Perez-Mayoral, Z. Musilova, B. Gil, B. Marszalek, M. Polozij, P. Nachtigall and J. Cejka, *Dalton Trans.*, 2012, **41**, 4036–4044.
10 L. Mitchell, B. Gonzalez-Santiago, J. P. S. Mowat, M. E. Gunn, P. Williamson, N. Acerbi, M. L. Clarke and P. A. Wright, *Catal. Sci. Technol.*, 2013, **3**, 606–617.
11 S. Marx, W. Kleist and A. Baiker, *J. Catal.*, 2011, **281**, 76–87.
12 K. Peikert, F. Hoffmann and M. Fröba, *Chem. Commun.*, 2012, **48**, 11196–11198.
13 O. Kozachuk, I. Luz, F. X. Llabres i Xamena, H. Noei, M. Kauer, H. B. Albada, E. D. Bloch, B. Marler, Y. Wang, M. Muhler and R. A. Fischer, *Angew. Chem., Int. Ed.*, 2014, **53**, 7058–7062.
14 O. Kozachuk, K. Yusenko, H. Noei, Y. Wang, S. Walleck, T. Glaser and R. A. Fischer, *Chem. Commun.*, 2011, **47**, 8509–8511.
15 F. Gul-E-Noor, B. Jee, M. Mendt, D. Himsl, A. Poeppl, M. Hartmann, J. Haase, H. Krautscheid and M. Bertmer, *J. Phys. Chem. C*, 2012, **116**, 20866–20873.
16 B. Jee, P. S. Petkov, G. N. Vayssilov, T. Heine, M. Hartmann and A. Pöppl, *J. Phys. Chem. C*, 2013, **117**, 8231–8240.
17 B. Jee, M. Hartmann and A. Pöppl, *Mol. Phys.*, 2013, **111**, 2950–2966.
18 J. Singh, C. Lamberti and J. A. van Bokhoven, *Chem. Soc. Rev.*, 2010, **39**, 4754–4766.
19 M. Bauer, C. Gastl, C. Köppl, G. Kickelbick and H. Bertagnolli, *Monatsh. Chem.*, 2006, **137**, 567–581.
20 A. B. Ene, M. Bauer, T. Archipov and E. Roduner, *Phys. Chem. Chem. Phys.*, 2010, **12**, 6520–6531.
21 S. Gross and M. Bauer, *Adv. Funct. Mater.*, 2010, **20**, 4026–4047.
22 M. A. Gotthardt, A. Beilmann, R. Schoch, J. Engelke and W. Kleist, *RSC Adv.*, 2013, **3**, 10676–10679.
23 K. C. C. Kharas, D. J. Liu and H. J. Robota, *Catal. Today*, 1995, **26**, 129–145.
24 L. S. Kau, D. J. Spirasolomon, J. E. Pennerhahn, K. O. Hodgson and E. I. Solomon, *J. Am. Chem. Soc.*, 1987, **109**, 6433–6442.

25 E. Borfecchia, S. Maurelli, D. Gianolio, E. Groppo, M. Chiesa, F. Bonino and C. Lamberti, *J. Phys. Chem. C*, 2012, **116**, 19839–19850.
26 C. Prestipino, L. Regli, J. G. Vitillo, F. Bonino, A. Damin, C. Lamberti, A. Zecchina, P. L. Solari, K. O. Kongshaug and S. Bordiga, *Chem. Mater.*, 2006, **18**, 1337–1346.
27 J. L. DuBois, P. Mukherjee, A. M. Collier, J. M. Mayer, E. I. Solomon, B. Hedman, T. D. P. Stack and K. O. Hodgson, *J. Am. Chem. Soc.*, 1997, **119**, 8578–8579.
28 S. Altwasser, R. Gläser, A. S. Lo, P. H. Liu, K. J. Chao and J. Weitkamp, *Microporous Mesoporous Mater.*, 2006, **89**, 109–122.